International Journal of Thermophysics, Vol. 23, No. 1, January 2002 (© 2002)

Effect of Processing Variables on the Structural Evolution of Silica Gels[1]

E. Drabarek,[2] J. R. Bartlett,[2,3] H. J. M. Hanley,[4,5] J. L. Woolfrey,[2] and C. D. Muzny[4]

Constant shear rate and dynamic rheological measurements have been used to investigate the effect of shear on the processes controlling the structural evolution (size and volume fraction of clusters and the extent of cluster–cluster cross-linking) during the gelation of colloidal silica sols. In the absence of shear, the storage and loss moduli (G' and G'', respectively) initially increase slowly prior to gelation, indicating that cluster growth and network formation are initially proceeding slowly, but then the system evolves rapidly, with cluster growth occurring at a slightly faster rate than network formation. In contrast, sols presheared for 4 h prior to gelation exhibit rapid increases in both G' and G'' immediately after cessation of the applied shear, reflecting significant differences in the evolution of the gel structure. On aging, the viscoelastic properties of the unsheared and presheared samples are similar, indicating that their structures are comparable on the length scales (several microns) being probed by the frequency range used here. However, their chemical and microstructural properties differ significantly, due to differences in the intercluster bonds. The effect of shear rate, initial pH, colloid particle size, and volume fraction on the structure of the resulting sols and gels is discussed.

KEY WORDS: gelation mechanism; gel point; gel structure; restructuring; rheology; silica; viscosity; viscoelasticity.

[1] Paper presented at the Fourteenth Symposium on Thermophysical Properties, June 25–30, 2000, Boulder, Colorado, U.S.A.

[2] Materials Division, Australian Nuclear Science and Technology Organization, Private Mail Bag 1, Menai NSW 2234, Australia.

[3] To whom correspondence should be addressed. E-mail: jxb@ansto.gov.au

[4] Physical and Chemical Properties Division, National Institute of Standards and Technology, Boulder, Colorado 80303, U.S.A.

[5] Executive, Australian Nuclear Science and Technology Organization, Private Mail Bag 1, Menai NSW 2234, Australia.

0195-928X/02/0100-0145/0 © 2002 Plenum Publishing Corporation

1. INTRODUCTION

Sol-gel processing has developed a variety of chemical techniques for controlling the solution chemistry and gelation environment [1], enabling the properties of ceramic products to be engineered for specific applications. However, the influence of macroscopic processing parameters, such as applied shear, has received far less attention. Since key properties of green ceramic bodies, including density, pore volume, and size distribution, are controlled by the structure of the sols and wet precursor gels, it is important to understand how structure evolves during the sol-to-gel transition. Rheological techniques are particularly appropriate for investigating the structure and texture of complex viscoelastic systems, such as those formed during sol-gel processing, since they measure characteristics of both elastic solids and viscous fluids [2].

In a previous study, we reported a simultaneous, *in situ* SANS/rheology study of the effect of applied shear on the rheological properties and structure of species formed during the sol-gel transition in concentrated colloidal silica (8-nm particle size) at pH 8 [3]. As the system gelled under a constant shear rate, the viscosity at first increased, then peaked when the shear stress reached a shear-rate-independent threshold, and, finally, decreased monotonically to $\sim$10% of the peak value. This low viscosity state could be maintained apparently indefinitely by continuous application of shear, but the system gelled once the shear was removed. It was demonstrated [3] that the gelling clusters densified when the critical shear stress was reached, leading to a significant decrease in the effective volume fraction of the clusters and a corresponding decrease in the viscosity. This structural densification was also accompanied by an abrupt increase in the size of the clusters, from $\sim$50 nm just before the viscosity peak to 500 to 1000 nm after the peak. In contrast, no such increase was observed in the absence of shear, with the final cluster size being $\sim$50 nm. The fractal dimensions of the clusters formed in the sheared and unsheared systems were 2.4 and 1.4, respectively, on SANS length scales of $\sim$1 to 500 nm. Subsequent studies of this system employed continuous oscillatory experiments to investigate further the evolution of the structure of silica gels obtained from unsheared and presheared sols at pH 8 [4, 5], extending the length scales over which the gel structure was investigated from $<$1 μm (SANS) to several microns (rheology).

Here we employ constant-shear rate and continuous oscillatory experiments to investigate the effect of colloid particle size, pH, and constant shear rate on the evolution of structure during the sol-to-gel transition in colloidal silica systems.

Table I. Selected Properties of Colloidal Silica Sols

Sol	Particle size (nm)	pH	Volume fraction (dry weight basis)
SM-30	7	9.9	0.17
HS-40	12	9.7	0.22
TM-50	21	9.0	0.30

2. EXPERIMENTAL

2.1. Materials and Gel Preparation

All gels were prepared from stock aqueous sols of commercial-grade Ludox silica (SM-30, HS-40, and TM-50 [6]); selected properties of the sols are given in Table I. In a typical experiment, the precursor sol was filtered using a 0.45-μm membrane to remove any large aggregates, and gelation was initiated by adding the required quantity of a standardized HCl solution ($\sim$5.0 mol·dm^{-3}) to 10.0 cm^3 of the filtered sol [3] to achieve a pH of 6.0 or 8.0. The resulting mixture was agitated vigorously for $\sim$30 s, then allowed to gel.

2.2. Rheology

The rheological properties of the gelling systems were investigated at 298 K, using a Haake CS-150 controlled stress rheometer [6]. The acid-treated sols were transferred to a thermostatted couette cell (used in conjunction with a solvent trap to minimize evaporation from the samples), with a sufficiently large gap (850 μm) to permit uniform growth of large agglomerates.

The evolution of structure as a function of shear rate was investigated by applying constant shear rates between 250 and 1400 s^{-1} (at 298 K) and measuring the corresponding shear stress as a function of reaction time. The viscoelastic properties of the evolving systems were investigated as follows.

- In the first series of experiments, gelation was allowed to proceed with a constant strain (γ) of 0.01 applied to the sample at an angular frequency (ω) of 6.28 rad·s^{-1} (1 Hz), and the storage/elastic and loss/viscous moduli (G' and G'', respectively) were measured as a function of time. Alternatively, a frequency sweep ($\omega = 0.1$ to 100 rad·s^{-1}), at the constant γ was applied to the samples. Data were

obtained at six discrete frequencies per decade, with a delay of 1 s between consecutive measurements.

- In the second series of experiments, the acidified sols were initially subjected to a constant shear rate of 500 s^{-1} for 4 h. The shear was then turned off and the oscillatory measurements were carried out on this presheared sample.

2.3. Quasi-Elastic Light Scattering

The apparent diffusion coefficient of the clusters in the unsheared, acidified sols was measured *in situ* via quasi-elastic light scattering, using a NICOMP Model 170 computing autocorrelator, interfaced, via fiber optics, to a Wyatt Technology DAWN DSP static light scattering system (configured with an Ar^+ laser) [6]. The samples were maintained at a temperature of 298 K within the DAWN DSP's sample compartment, and scattering was monitored at an angle of 79.5° to the incident 488.0-nm beam.

3. RESULTS AND DISCUSSION

3.1. Effect of Shear on Kinetics and Gel Structure

Typical variation in G' and G'' with time during the gelation of the unsheared system at $\omega = 6.28$ rad$\cdot s^{-1}$ and $\gamma = 0.01$ is shown in Fig. 1. Also included are the moduli for the system presheared for 4 h at 500 s^{-1}. The corresponding values of G' and G'' differ at times less than the crossover time, t_x. In particular, t_x occurs much earlier in the sheared sample (2150 s, presheared; 4250 s, unsheared), and the values of G' and G'' for the unsheared sample both exhibit an apparent plateau until $\sim$3000 s has elapsed after initiating gelation. In contrast, no such plateau is observed for the presheared system.

To a first approximation, the evolution of G'' (i.e., the viscous component) reflects variations in the size and volume fractions of the growing clusters in the gelling system [7, 8]. Conversely, the evolution of G' (i.e., the solid-like component) is related to the extent of the cluster–cluster interpenetration and cross-linking. For the unsheared gel, the plateau behaviour of G' and G'' prior to t_x thus suggests that cluster growth and network formation are initially proceeding slowly, but then the system changes rapidly, with cluster growth occurring at a slightly faster rate than networking. In contrast, for the presheared gel, both mechanisms appear to occur immediately after the cessation of the applied shear. However,

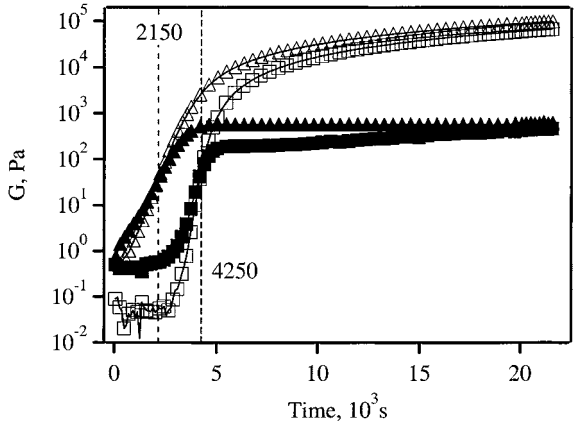

Fig. 1. Variations in G'' and G' with time for unsheared and presheared (500 s^{-1}, 4 h) sols. □, G' (unsheared); ■, G'' (unsheared); △, G' (presheared); ▲, G'' (presheared). Frequency, 6.28 rad·s^{-1}; strain, 0.01.

the rate of increase in G' and G'' before t_x is significantly higher for the unsheared sol, reflecting a higher rate of cross-linking and interpenetration for the latter sample once a population of clusters has formed. Indeed, once the unsheared clusters have formed during the plateau phase, they gel more rapidly (i.e., within ~1200 s) than those formed by preshearing (which require ~2150 s to form a gel).

For times greater than t_x, each set of curves superficially appears to scale with respect to their respective values of t_x. Also, the corresponding curves merge at the asymptotic time limit. However, it is seen that the values of G'' for the presheared sample reach a plateau relatively soon after t_x is reached, whereas G'' for the unsheared sample increases more slowly. One can surmise that clusters in the unsheared system are still evolving after t_x, but those in the presheared system do not grow significantly. Furthermore, prior to extended aging, the volume fraction of solids in the gel matrices prepared in this study are relatively low ($\phi = 0.17$), and the freshly formed networks typically contain large, interconnected cavities filled with solvent. The mobile solvent phase can contain dissolved species and small particles or clusters that have not attached to the percolating network. The monotonic increase in G'' after the gel point for the unsheared system suggests that such species are present in the mobile phase and that they aggregate with clusters that are already part of the evolving network. No such effect is observed for the sheared system, presumably because densification of the clusters limits this effect.

Further differences between the unsheared and the presheared gels are observed from the plots of the frequency sweeps. As is well known, both G' and G'' can exhibit a power law dependence on applied frequency [9, 10],

$$G' \sim \omega^{n_1} \tag{1}$$

and

$$G'' \sim \omega^{n_2} \tag{2}$$

where n_i, the viscoelastic exponents, reflect the rigidity of the gel. At the gel-point time (t_{gel}), $n_1 = n_2 = n_{gel}$, and the power-law plots for G' and G'' are parallel and, possibly, coincident. Variations in G' and G'' with applied frequency near the gel point are illustrated in Fig. 2 for the unsheared sols (the presheared sols showed similar trends). Both systems fulfill the criteria that $n_1 = n_2 = n_{gel}$, where the G' and G'' power-law plots are superimposed at the gel point. Hence, to a first approximation, $t_x \approx t_{gel}$.

We have also confirmed the equivalence of t_x and t_{gel} by investigating variations in the apparent diffusion coefficient (D) of the clusters in the unsheared system with time, using quasi-elastic light scattering (Fig. 3). These data clearly indicate that D begins to decrease rapidly at t_x, consistent with the onset of gelation.

The viscoelastic exponent for the presheared system (0.45) was significantly higher than that for the unsheared sample (0.27), indicating

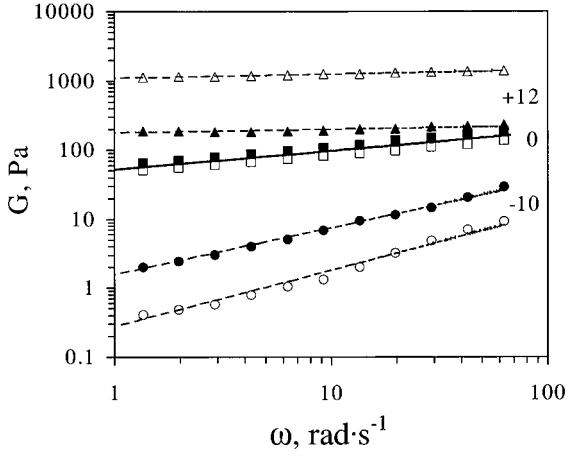

Fig. 2. Frequency dependence of G' and G'' for unsheared sol at or near t_x, defined as the time at which $G' = G''$. Solid symbols, G''; open symbols, G'. (●, ○), 10 min before gel point; (■, □) gel point; (▲, △) 12 min after gel point.

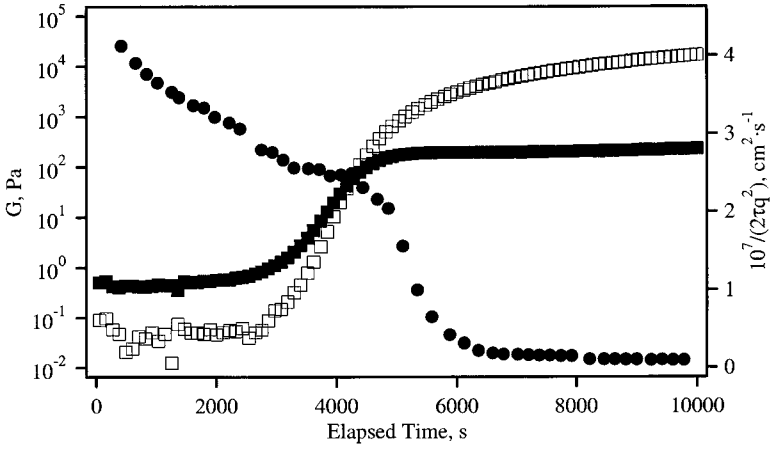

Fig. 3. Variations in G'' (■), G' (□), and apparent diffusion coefficient (●) with time for an unsheared sol. Oscillation frequency, 6.28 rad·s^{-1}; strain, 0.01.

that the presheared gel is more viscoelastic (i.e., less elastic) at the gel point and for many minutes after t_{gel}. Similarly, the value of G'/G'' at t_{gel} for the unsheared sample (51 Pa) was significantly higher than the corresponding value for the presheared system (25 Pa). These data suggest that the unsheared gel has a more strongly cross-linked structure than the presheared system at t_{gel}.

The asymptotic behaviour of the moduli indicates that the structures of the final wet gels are comparable, on the length scale of several microns probed by the frequency range used here. However, the chemical and microstructural properties are significantly different [4, 5]. The unsheared gels (both wet and dried at ambient temperature) are completely transparent, whereas the corresponding presheared gels are translucent. This is consistent with the known cluster sizes in the respective gels (~50 and 700 nm, respectively, as determined by quasi-elastic light scattering and SANS Guinier extrapolation [3]). Further, the presheared gel can be redispersed in either water or an electrolyte with an ionic strength comparable to that of the parent sol, for at least 16 h after gelation. In contrast, samples of the unsheared gel that have been aged for 4 h will not disperse in the electrolyte solution, although they can be dispersed in water. However, aging unsheared gels for 8 h renders them nondispersible in water.

A logical interpretation of these results is that the intercluster bonds in the presheared sample consist mainly of hydrogen bonds, whereas the unsheared gels initially consist of a mixture of hydrogen and siloxane

bonds. Hydrogen bonds can be readily cleaved by hydrolysis (enabling the networked clusters to be deaggregated), while the siloxane bonds resist such cleavage. Both the 50- and the 700-nm clusters in the unaged gels are capable of dispersing in water, due to the relatively high barrier to aggregation under such low-ionic strength conditions [1]. However, the 50-nm clusters (unsheared gel) have a relatively low barrier to aggregation in the strong electrolyte, and hence, reaggregation occurs rapidly. The 700-nm clusters (presheared gel) are significantly more stable in strong electrolytes, and the presheared gel can thus disperse in the presence of a strong electrolyte background. Finally, gel aging converts the intercluster hydrogen bonds to siloxane bonds, leading to the formation of a nondispersible product. A simple model [11] suggests that these chemical effects are directly related to the different aggregate structures formed in the unsheared and presheared systems and the corresponding differences in the abundances of surface hydroxyls available for cross-linking and formation of stable siloxane bonds.

3.2. Effect of Particle Size on Gelation

Variations in the shear stress of the 12- and 21-nm sols at pH 6, and a constant volume fraction and shear rate (0.22 and 1000 s^{-1}, respectively), are shown in Fig. 4. As the acidified sols aggregate and form extended networks under a constant shear rate, their viscosities first increase, then peak when the shear stress reaches a critical threshold, and, finally,

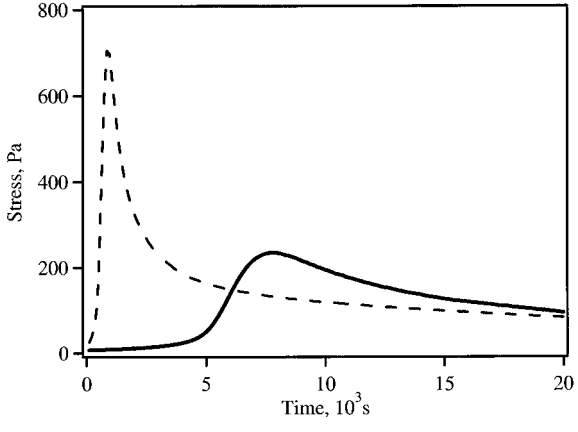

Fig. 4. Variations in shear stress for the 12-nm (- - - -) and 21-nm (——) sols with time, at a constant shear rate of 1000 s^{-1} (pH 6, $\phi = 0.22$).

Table II. Selected Properties of Gels

Particle diameter (nm)	Surface hydroxyls per unit volume	Gel time (s)	Moduli at t_x (Pa)	pH of acidified precursor sol
7	3.4	4,250	50	8
7	3.4	180	23	6
12	2.0	5,840	5.0	6
21	1.0	29,400	1.9	6

decreased monotonically to ~10% of the peak values. A similar qualitative trend was reported earlier for a 7-nm silica sol (Ludox SM-30 [3, 6]). In the latter case, it was demonstrated that the growing clusters densified when a critical shear stress was reached, leading to a significant decrease in the effective volume fraction of the clusters and a corresponding decrease in the viscosity. Inspection of Fig. 4 reveals that an increase in the particle size leads to an increase in the time required for the system to achieve a critical stress (t_{crit}) and to a corresponding decrease in the magnitude of the peak stress (τ_{crit}).

- The increase in t_{crit} with increasing particle size (12 nm, $t_{crit} = 870$ s; 21 nm, $t_{crit} = 7800$ s) is attributed to the lower concentration of surface hydroxyl species in the latter system (Table II), which leads to a corresponding decrease in the rate of network formation from the law of mass action.
- The decrease in τ_{crit} with increasing particle size (12 nm, $\tau_{crit} \sim 710$ Pa; 21 nm, $\tau_{crit} = 240$ Pa) is similarly attributed to the lower abundance of surface hydroxyl species in the latter system. A decrease in the concentration of surface hydroxyl species would be expected to lead to a decrease in the number of siloxane bonds formed during the evolution of the gel structure and to an associated decrease in the strength of the interparticle network. Hence, we would expect a corresponding decrease in the maximum shear stress that the network could sustain prior to restructuring, leading to a lower critical stress, as is observed experimentally. A quantitative study of the effect of volume fraction on τ_{crit} will be reported in a future study.

The effect of particle size (7, 12, and 21 nm) at a fixed volume fraction (0.17) and pH (6.0) on the temporal evolution of G' and G'' is presented in Table II and Fig. 5. Also included in Table II are the relative numbers of surface hydroxyl species per unit volume, estimated from the nominal surface areas of the particles. Increasing particle size leads to an increase in

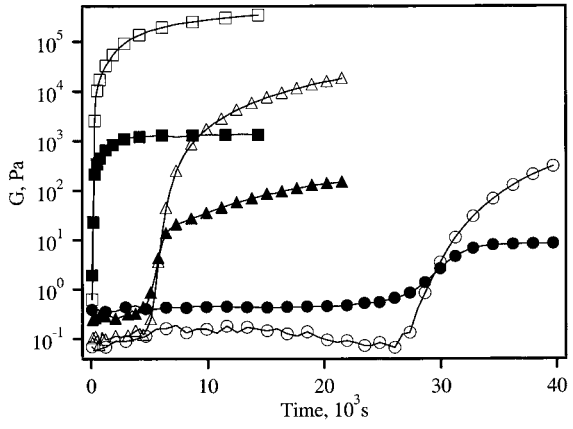

Fig. 5. Variations in G'' and G' with time during gelation of the sols at pH 6. Solid symbols, G''; open symbols, G'. (■, □) 7-nm particles; (▲, △) 12-nm particles; (●, ○) 21-nm particles. Frequency, 6.28 rad·s^{-1}; strain, 0.01.

t_{gel} and to a corresponding decrease in the value of G'/G'' (network strength) at t_{gel}. The effect of particle size on t_{gel} is attributed to the number of surface hydroxyl species available for network formation in these systems, on the basis of the simple, semiquantitative treatment below.

To a first approximation, the principal reactions leading to formation of the gel network at a given time may be represented by the following simplified scheme.

$$\text{—SI—OH} + \text{OH—SI—} \longrightarrow \text{—SI—O(H)—Si—} \qquad (3)$$

where the Si–O(H)–Si bonds may be either siloxane bonds or hydroxyl bridges. If the concentration of surface hydroxyl species is given by H, then the rate of gelation (network formation) at any given pH is

$$\frac{d(H)}{dt} = -kH^2 \qquad (4)$$

or

$$kt = \frac{1}{H_t} - \frac{1}{H_0} \qquad (5)$$

where k and H_i are the rate constant and concentration of surface hydroxyl species at time i. At t_{gel}, $H_t = H_{t_{gel}}$, and Eq. (5) may be rewritten

$$kt_{gel} = \frac{1}{H_{t_{gel}}} - \frac{1}{H_0} \tag{6}$$

If it is assumed that the number of hydroxyls per unit volume involved in forming the gel network, $H_{network}$, is essentially independent of particle size, then

$$H_{t_{gel}} = H_0 - H_{network} \tag{7}$$

and

$$kt_{gel} = \frac{1}{H_0 - H_{network}} - \frac{1}{H_0} \tag{8}$$

Variations in t_{gel} with $(H_0)^{-1}$, and the corresponding least-squares fit using Eq. (8) ($k = 6.2 \times 10^{-5}$; $H_{network} = 0.65$; $R^2 = 0.996$) are shown in Fig. 6. Ratioing the relevant hydroxyls per unit volume (Table II) with $H_{network}$ suggests that ~65% of the available surface hydroxyl species are involved in network formation in the case of the 21-nm particles, whereas only ~20% are consumed at t_{gel} in the case of the 7-nm particles. These data enable two independent tests of the model to be undertaken.

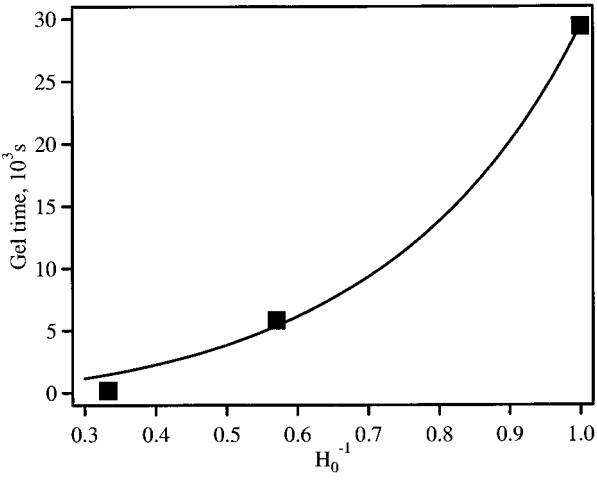

Fig. 6. Dependence of t_{gel} on H_0. The solid line is the least-squares fit of Eq. (8) to the data, with $k = 6.2 \times 10^{-5}$ and $H_{network} = 0.65$ ($R^2 = 0.996$).

- In both the 7- and the 21-nm systems, the availability of additional reaction sites after formation of the initial gel network would imply that the strength of the networks should increase during subsequent aging, as dissolved species and small mobile clusters initially present in the solvent phase attach to the evolving gel network. Such effects are clearly evident from Fig. 5, where the values of G' approach asymptotic values of $\sim 4 \times 10^5$ and 1.4×10^4 Pa for gels obtained from the 7- and 21-nm particles, respectively.

- In addition, the fact that up to $\sim 80\%$ of the sites initially available for network formation remain unreacted at t_{gel} for the 7-nm system, whereas only $\sim 35\%$ remain unreacted in the 21-nm system, would imply that the magnitude of G' should increase by a greater factor in the former system during aging. Again, such an effect is clearly evident in Fig. 5. In particular, G' increased by a factor of $\sim 17{,}000$ during aging in the 7-nm system but by only ~ 7400 in the 21-nm system.

3.3. Effect of pH

The effect of pH on the stability of gelation of colloidal silica sols has been investigated in detail [12]. It is well known that the maximum gelation rate is observed near pH 6, with the rate decreasing significantly at higher and lower pH levels. This effect is clearly shown in Fig. 7, which compares the evolution of the loss and elastic moduli with time for the 7-nm system at pH 6 and 8. As expected, the value of t_{gel} at pH 6 (180 s) is significantly less than that at pH 8 (4250 s). However, it is also evident (Table II) that the strength of the gel network formed at pH 8 (50 Pa, determined from the value of G'/G'' at t_{gel}) is substantially higher than that obtained at pH 6 (23 Pa).

Healy [13] has presented a qualitative model of the surface speciation of colloidal silica as a function of pH and its effect on the particle–particle interaction potentials (V) as a function of particle separation distance (R). A key postulate of this model is that silica particles are stabilized by a sorbed layer of polysilicate species at pH < 10.5 and that coagulation/gelation at ionic strengths exceeding a critical, pH-dependent value is due to the presence of a secondary minimum in the V–R diagram under such conditions. The polysilicate layer functions as an ion exchanger, and its thickness increases with decreasing pH (due to conversion of $\equiv$Si–O^- sites to $\equiv$Si–OH species) and decreasing ionic strength (for instance, due to conversion of $\equiv$Si–O^-Na^+ sites to $\equiv$Si–O^- sites [13]).

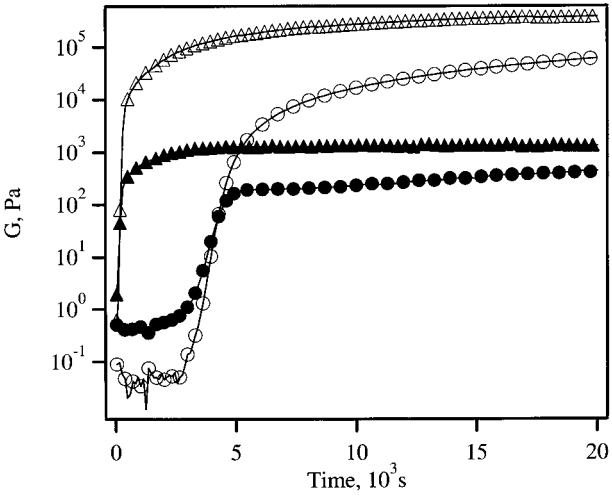

Fig. 7. Time evolution of G'' and G' during gelation of the 7-nm system, as a function of the initial pH. Solid symbols, G''; open symbols, G'. (▲, △), pH 6; (●, ○) pH 8. Frequency, 6.28 rad·s^{-1}; strain, 0.01.

The initial conductivity of the stable SM-30 sol (pH 9.8) was found to be 7.5 mS·cm^{-1}, which is equivalent to an initial [Na^+] of ~0.13 mol·dm^{-3} in the solution phase (excluding that which may be sorbed on the polysilicate layer). The addition of sufficient HCl to adjust the pH of the sol to either 8 or 6 (which requires 1.4 and 2.1 mmol, respectively, of the acid for 10 cm^3 of the sol) would clearly increase the ionic strength substantially, to values well in excess of the electrolyte concentrations required to induce secondary minima in the V–R diagrams [13]. Hence, the evolution of a gel network in both the pH 6 and the pH 8 systems was expected to occur initially through van der Waals interactions within the secondary minima, with aggregation and cluster formation occurring more chaotically in the former case. The subsequent development of a "strong" network occurs through the formation of hydroxyl bridges or siloxane bonds (i.e., ≡Si–O(H)–Si≡ species) between adjacent clusters and particles. It was anticipated that relatively large values of t_{gel}, as observed at pH 8, would enable restructuring to occur during formation of the ≡Si–O(H)–Si≡ groups, thus maximizing the number of such strong interparticle bonds produced during evolution of the gel network. Conversely, shorter values of t_{gel} (pH 6) would reduce the time available for such restructuring, leading to a reduction in the number of such bonds, and to a

corresponding reduction in the strength of the network formed at t_{gel}, as is observed experimentally.

Although the strength of the freshly formed gel network (t_{gel}) at pH 8 is higher than that obtained at pH 6 [$\sim 7 \times 10^4$ Pa for pH 8; $\sim 4 \times 10^5$ Pa for pH 6 (Fig. 7)], this trend is reversed at times immediately after t_{gel} and on extended aging, with the pH 6 network approaching asymptotic strengths that are significantly higher than those observed at pH 8 ($\sim 7 \times 10^4$ Pa, pH 8; $\sim 4 \times 10^5$ Pa, pH 6). Two explanations for this effect have been considered.

- Formation of ≡Si–O(H)–Si≡ bonds can occur only by reaction between two adjacent ≡Si–OH species (and elimination of a water molecules) or by a nucleophilic substitution reaction involving ≡Si–OH and ≡Si–O^- sites (and elimination of an $[OH]^-$ ion). No such reaction is possible between two ≡Si–O^- sites. Since the relative abundance of ≡Si–OH sites in the pH 6 system is higher than that at pH 8, a greater number of ≡Si–O(H)–Si≡ bonds is expected in the former system, leading to a corresponding increase in the strength of the aged network, as is observed experimentally.
- An increase in the rate of formation of the gel network (decreasing t_{gel}) is expected to result in an increase in the probability of unreacted monomers and small clusters being trapped in the mobile solvent phase at t_{gel}. These monomers and clusters can then react with the gel framework during subsequent aging, leading to an increase in the strength of the aged network. The magnitude of the increase is expected to increase with decreasing t_{gel}, consistent with the relative strengths of the aged networks obtained at pH 6 and 8.

Both explanations qualitatively account for the observed data.

4. CONCLUSIONS

Constant-shear rate and continuous oscillatory experiments have been used to investigate the effect of colloid particle size, pH, and shear rate on the evolution of structure (size and volume fraction of clusters and extent of cluster–cluster cross linking) during the sol-to-gel transition in colloidal silica systems.

1. As colloidal silica sols gel, aggregating and forming extended networks, under a constant shear rate, their viscosities at first increase, then peak when the shear stress reaches a critical threshold (t_{crit}), and, finally, decrease monotonically to ~10% of the peak values.

2. In the absence of shear, the G' and G'' moduli increase slowly prior to gelation, indicating that cluster growth and network formation initially proceed slowly, but then the system evolves rapidly, with cluster growth occurring at a slightly faster rate than network formation. In contrast, sols presheared prior to gelation exhibit rapid increases in both G' and G'' immediately after cessation of the applied shear, reflecting significant differences in evolution of the gel structure.
3. On aging, the viscoelastic properties of the unsheared and presheared samples are similar, indicating that their structures are comparable on the length scale of several microns being probed by the frequency range used here. However, their nanostructures and chemical properties differ significantly, due to differences in the internal (i.e., submicron) structure of the aggregates and the interaggregate bonds.
4. An increase in the particle size of the colloids leads to an increase in the time required for the system to achieve a critical stress (t_{crit}) and to a corresponding decrease in the magnitude of the peak stress (τ_{crit}). This is attributed to the lower abundance of surface hydroxyl species with increasing particle size and their associated influence on the gelation mechanism.
5. Increasing pH increases the gelation time and reduces the strength of the aged gel network. This is interpreted in terms of the effect on bonding reactions in the gel structure.

REFERENCES

1. C. J. Brinker and G. W. Scherer, *Sol-Gel Science, The Physics and Chemistry of Sol-Gel Processing* (Academic Press, San Diego, 1990).
2. A. Wineman, *Mater. Res. Bull.* **XVI-8**:19 (1991).
3. H. J. M. Hanley, C. D. Muzny, B. D. Butler, G. C. Straty, J. R. Bartlett, and E. Drabarek, *J. Phys. Condens. Matter* **11**:1369 (1999).
4. E. Drabarek, J. R. Bartlett, H. J. M. Hanley, J. L. Woolfey, and C. D. Muzny, *J. Sol-Gel Sci. Technol.* (in press).
5. E. Drabarek, J. R. Bartlett, H. J. M. Hanley, J. L. Woolfey, and C. D. Muzny, *Proceedings of the XIII International Congress on Rheology*, Cambridge, UK, 20–25 August (2000).
6. The trade names Ludox SM-30, HS-40 and TM-50, Haake, NICOMP, and Wyatt Technology are noted to allow the experiment to be reproduced exactly. Their use does not imply endorsement by NIST.
7. B.Cabane, M. Dubois, and B. Duplessix, *J. Phys.* **48**:2131 (1987).
8. M. Dubois and B. Cabane, *Macromolecules* **22**:2526 (1989).
9. M. Mathukumar, *J. Chem. Phys.* **83**:3161 (1985).

10. M. Mathukumar, *Macromolecules* **22**:4656 (1989).
11. E. Drabarek, J. R. Bartlett, H. J. M. Hanley, J. L. Woolfey, and C. D. Muzny, in preparation.
12. R. K. Iler, in *The Chemistry of Silica. Solubility, Polymerisation, Colloid and Surface Properties, and Biochemistry* (John Wiley, New York, 1979).
13. T. W. Healy, in *The Colloid Chemistry of Silica*, H. E. Bergna, ed. (Am. Chem. Soc., Washington, DC, 1994), p. 147.